Dirac spectrum and the BEC-BCS crossover in QCD at nonzero isospin asymmetry

Francesca Cuteri

in collaboration with Gergely Endrődi, Bastian Brandt, Sebastian Schmalzbauer

Theory of Hadronic Matter Under Extreme Conditions II
Dubna, September 16, 2019

Outline

1. QCD with isospin
2. The phase diagram of QCD with isospin on the lattice
3. Signatures of the BCS phase at high μ_I
4. Results

QCD WITH ISOSPIN

[Physical motivation, numerical advantages,

analytic results for the phase diagram]

Motivation

A nonzero isospin density $n_\mathrm{I} = n_\mathrm{u} - n_\mathrm{d}$ describes an asymmetry between the densities of up and down quarks

- hence between the densities of protons and neutrons

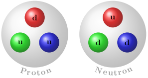

- hence between the densities of π^+ and π^-

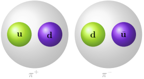

Motivation

A nonzero isospin density $n_\mathrm{I} = n_\mathrm{u} - n_\mathrm{d}$ describes an asymmetry between the densities of up and down quarks

- hence between the densities of protons and neutrons

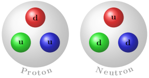

- hence between the densities of π^+ and π^-

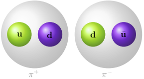

The $n_\mathrm{I} < 0$ case is relevant for

- the initial state of heavy ion collisions
  - imbalance between produced charged pions

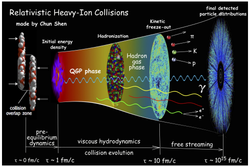

- structure of cold neutron stars
  - very low proton fraction

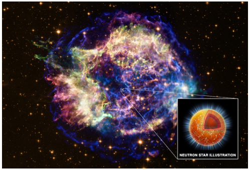

Isospin chemical potential

Consider QCD with three flavors of fermions in the grand canonical ensemble, where quark chemical potentials are the conjugated quantities to the quark densities

$$\mu_{\mathrm{u}} = \frac{\mu_{\mathrm{B}}}{3} + \mu_{\mathrm{I}}, \qquad \mu_{\mathrm{d}} = \frac{\mu_{\mathrm{B}}}{3} - \mu_{\mathrm{I}}, \qquad \mu_{\mathrm{s}} = \frac{\mu_{\mathrm{B}}}{3} - \mu_{\mathrm{S}}$$

- Consider zero baryon number and strangeness, but nonzero isospin

$$\mu_{\mathrm{B}} = 0, \qquad \mu_{\mathrm{S}} = 0, \qquad \mu_{\mathrm{I}} = \mu_{\mathrm{u}} = -\mu_{\mathrm{d}}$$

- One can then define a pion chemical potential $\mu_\pi = \mu_{\mathrm{u}} - \mu_{\mathrm{d}} = 2\mu_{\mathrm{I}}$ to which corresponds the isospin density $n_{\mathrm{I}} = n_{\mathrm{u}} - n_{\mathrm{d}}$

Chemical potential & positivity of the measure

PHYSICAL REVIEW D, VOLUME 59, 054502

Imaginary chemical potential and finite fermion density on the lattice

Mark Alford, Anton Kapustin, and Frank Wilczek
School of Natural Sciences, Institute for Advanced Study, Princeton, New Jersey 08540
(Received 7 August 1998; published 29 January 1999)

Standard lattice fermion algorithms run into the well-known sign problem with a real chemical potential. In this paper we investigate the possibility of using an *imaginary* chemical potential and argue that it has advantages over other methods, particularly for probing the physics at finite temperature as well as density. As a feasibility study, we present numerical results for the partition function of the two-dimensional Hubbard model with an imaginary chemical potential. We also note that systems with a net imbalance of isospin may be simulated using a real chemical potential that couples to I_3 without suffering from the sign problem.

Alford, Kapustin, Wilczek (1999)

- Systems with net imbalance of isospin $n_I \neq 0$ can be simulated with standard Monte Carlo importance sampling techniques using $\mu_I \in \mathbb{R}$ that couples to $I_3 = \frac{\tau_3}{2}$!

QCD at finite isospin density

VOLUME 86, NUMBER 4 PHYSICAL REVIEW LETTERS 22 JANUARY 2001

QCD at Finite Isospin Density

D. T. Son[1,3] and M. A. Stephanov[2,3]
[1]*Physics Department, Columbia University, New York, New York 10027*
[2]*Department of Physics, University of Illinois, Chicago, Illinois 60607-7059*
[3]*RIKEN-BNL Research Center, Brookhaven National Laboratory, Upton, New York 11973*
(Received 31 May 2000)

QCD at finite isospin chemical potential μ_I has no fermion sign problem and can be studied on the lattice. We solve this theory analytically in two limits: at low μ_I, where chiral perturbation theory is applicable, and at asymptotically high μ_I, where perturbative QCD works. At low isospin density the ground state is a pion condensate, whereas at high density it is a Fermi liquid with Cooper pairing. The pairs carry the same quantum numbers as the pion. This leads us to conjecture that the transition from hadron to quark matter is smooth, which passes several tests. Our results imply a nontrivial phase diagram in the space of temperature and chemical potentials of isospin and baryon number.

Son, Stephanov (2001)

Non trivial phase diagram drawn on the basis of analytic computations in

- the $n_I \to 0$ limit $\longleftarrow$ Chiral Perturbation Theory
- the $n_I \to \infty$ limit $\longleftarrow$ Perturbative QCD

QCD at finite isospin density - The $n_I \to 0$ limit from χPT

- **In the limit $|\mu_I| \ll m_\rho$ χPT applies**
- Charged pions are the lightest hadrons that couple to the isospin chemical potential. χPT describes their effective dynamics
- At $T = 0$, if the isospin chemical potential exceeds the critical value $\mu_{I,c} = m_\pi/2$, sufficient energy is pumped into the system so that charged pions can be created
- Due to the bosonic nature of pions, a Bose-Einstein condensate (BEC) is formed
- χPT also predicts that the transition between the vacuum and the BEC state is of second order with the universality class $\mathrm{O}(2)$

QCD at finite isospin density - The $n_I \to \infty$ limit from p-QCD

- **In the limit $|\mu_I| \gg \Lambda_{QCD}$ p-QCD applies**
- Perturbation theory predicts that the attractive gluon interaction forms Cooper-pairs (BCS superconductivity) of u and $\bar{d}$ quarks in the pseudoscalar channel
- Transition between the BEC and BCS states expected to be an analytic crossover since the resulting pair has the same quantum numbers as the pion condensate
- At asymptotically large μ_I, decoupling of the gluonic sector and emergence of a first-order deconfinement phase transition

QCD at finite isospin density - The “analytic phase diagram”

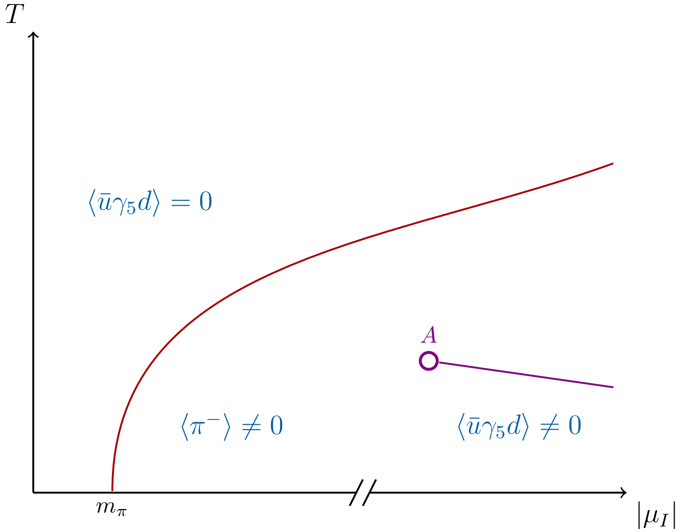

THE PHASE DIAGRAM OF QCD WITH ISOSPIN ON THE LATTICE

Brandt, Endrödi, Schmalzbauer (2018)

[Lattice setup, symmetry breaking patterns, Pion BEC, Pionic source λ, Chiral restoration, Order parameters]

N_I-QCD on the lattice - Setup

- QCD with $N_f = 2+1$ improved dynamical staggered quarks with physical quark masses at various T, μ_I and values of the I.R. regulator λ

$$S_{ud} = \bar{\psi}\mathcal{M}_{ud}\,\psi, \qquad \psi = (u,d)^\top,$$
$$\mathcal{M}_{ud} = \gamma_\mu(\partial_\mu + iA_\mu)\,\mathbb{1} + m_{ud}\mathbb{1} + \mu_I\gamma_4\tau_3 + i\lambda\gamma_5\tau_2\,,$$

- Explicit, unphysical symmetry breaking term in $\mathcal{M}_{ud}$ couples to the charged pion field $\pi^\pm$, the coupling λ referred to as "pionic source"

$$S_{ud} = S_{ud}(\lambda = 0) + \lambda\,\pi^\pm, \quad \pi^\pm \equiv \bar{\psi}i\gamma_5\tau_2\psi = \bar{u}\gamma_5 d - \bar{d}\gamma_5 u\,.$$

- $N_s^3 \times N_t$ lattices with spacing a, temperature $T = 1/(N_t a)$ and spatial volume $V = (N_s a)^3$, gauge coupling $\beta = 6/g^2$ and

$$\mathcal{Z} = \int \mathcal{D}U_\mu\, e^{-\beta S_G^{\mathrm{Sym}}}\,(\det\mathcal{M}_{ud})^{1/4}\,(\det\mathcal{M}_s)^{1/4}\,, \qquad U_\mu = \exp(iaA_\mu)$$

$\mathcal{M}_{ud}$ light quark matrix (in the u and d quarks basis), $\mathcal{M}_s$ s quark matrix.

n_I-QCD on the lattice - Symmetry breaking patterns

- $SU_V(2) \times U_V(1)$ flavor symmetry group for QCD with light quark matrix

$$\mathcal{M}_{ud}\big|_{\mu_i=\lambda=0} = \gamma_\mu(\partial_\mu + iA_\mu)\,\mathbb{1} + m_{ud}\mathbb{1}$$

- At $\mu_I \neq 0$ $\longrightarrow$ $\mathcal{M}_{ud} = \mathcal{M}_{ud}\big|_{\mu_i=\lambda=0} + \mu_I\gamma_4\tau_3$

$$SU_V(2) \times U_V(1) \longrightarrow U_{\tau_3}(1) \times U_V(1)$$

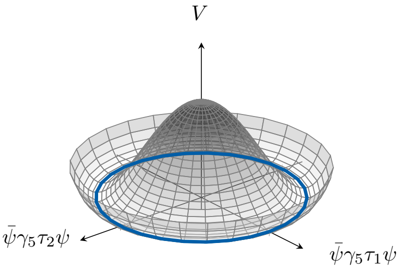

- **Spontaneous breaking** with pion condensate $\langle\bar\psi\gamma_5\tau_{1,2}\psi\rangle$
  $\longrightarrow$ Appearance of Goldstone mode

n_I-QCD on the lattice - Symmetry breaking patterns

- $SU_V(2) \times U_V(1)$ flavor symmetry group for QCD with light quark matrix

$$\mathcal{M}_{ud}\big|_{\mu_i=\lambda=0} = \gamma_\mu(\partial_\mu + iA_\mu)\,\mathbb{1} + m_{ud}\mathbb{1}$$

- At $\mu_I \neq 0$, $\lambda \neq 0$ $\longrightarrow$ $\mathcal{M}_{ud} = \mathcal{M}_{ud}\big|_{\mu_i=\lambda=0} + \mu_I\gamma_4\tau_3 + i\lambda\gamma_5\tau_2$

$$SU_V(2) \times U_V(1) \longrightarrow U_{\tau_3}(1) \times U_V(1) \longrightarrow \varnothing \times U_V(1)$$

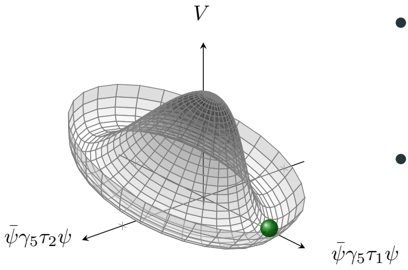

- **Spontaneous breaking** with pion condensate $\langle\bar\psi\gamma_5\tau_{1,2}\psi\rangle$
  $\longrightarrow$ Appearance of Goldstone mode

- **Explicit breaking** via pionic source λ,
  $\longrightarrow$ pseudo-Goldstone boson
  (λ necessary trigger for spontaneous breaking to occurr at finite V)

n_I-QCD on the lattice - Breaking of $U_{\tau_3}(1)$ symmetry

- Spontaneous, by $\langle \pi^\pm \rangle$, and explicit, by λ, breaking of the $\mathrm{U}_{\tau_3}(1)$ symmetry is completely analogous to the spontaneous, by $\langle \bar\psi\psi \rangle$, and explicit, by m_{ud} breaking of the standard chiral symmetry at $\mu_I = 0$

Pion condensation		**Chiral symmetry breaking**
$U_{\tau_3}(1) \to \varnothing$	$\xleftrightarrow{\text{breaking pattern}}$	$SU_L(2) \otimes SU_R(2) \to SU_V(2)$
1	$\xleftrightarrow{\#\text{ Goldstones}}$	3
$\langle \bar\psi \gamma_5 \tau_2 \psi \rangle$	$\xleftrightarrow{\text{condensates}}$	$\langle \bar\psi\psi \rangle$
$\lambda \to 0$	$\xleftrightarrow{\text{explicit breaking}}$	$m \to 0$
$\rho^{\lvert \not{D}(\mu_I) + m \rvert^2}(0)$	$\xleftrightarrow{\text{Banks-Casher}}$	$\rho^{(\not{D})}(0)$

- While in nature $m_{ud} > 0$, λ is unphysical: the limit $\lambda \to 0$ must be taken!

n_I-QCD on the lattice - Observables

- The pion condensate and quark condensate obtainable from $\mathcal{Z}$, via differentiation and measurable with noisy-estimator techniques

$$\left\langle \pi^{\pm} \right\rangle = \frac{T}{V}\frac{\partial \log \mathcal{Z}}{\partial \lambda} = \frac{T}{2V}\,\mathrm{tr}\,\frac{\lambda}{|\not{D}(\mu_I) + m_{ud}|^2 + \lambda^2}$$
$$\left\langle \bar{\psi}\psi \right\rangle = \frac{T}{V}\frac{\partial \log \mathcal{Z}}{\partial m_{ud}} = \frac{T}{2V}\,\mathrm{Re}\,\mathrm{tr}\,\frac{\not{D}(\mu_I) + m_{ud}}{|\not{D}(\mu_I) + m_{ud}|^2 + \lambda^2}$$

then becoming, after appropriate multiplicative/additive renormalization,

$$\Sigma_{\bar{\psi}\psi} = \frac{m_{ud}}{m_\pi^2 f_\pi^2}\left[\left\langle \bar{\psi}\psi \right\rangle_{T,\mu_I} - \left\langle \bar{\psi}\psi \right\rangle_{0,0}\right] + 1$$
$$\Sigma_{\pi} = \frac{m_{ud}}{m_\pi^2 f_\pi^2}\left\langle \pi^{\pm} \right\rangle_{T,\mu_I}$$

- The renormalized Polyakov loop $P_r(T,\mu_I) = Z \cdot \left\langle \frac{1}{V}\sum_{n_x,n_y,n_z} \mathrm{Tr} \prod_{n_t=0}^{N_t-1} U_t(n) \right\rangle$

with $Z = \left(\frac{P_\star}{P(T_\star,\mu_I=0)}\right)^{T_\star/T}$, and $T_\star = 162$ MeV, hence $P_\star = 1$

RESULTS

[Phase diagram in the $\mu_I - T$ plane, Chiral crossover, Pion condensation, Deconfinement, BCS phase]

n_I-QCD result for $\langle\pi^\pm\rangle$ and $\langle\bar\psi\psi\rangle$ - The $\lambda \to 0$ extrapolation

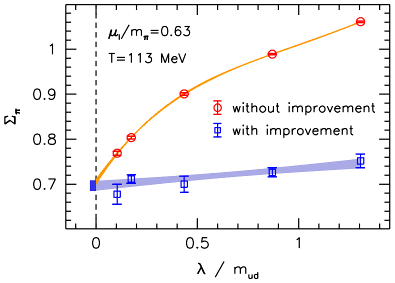

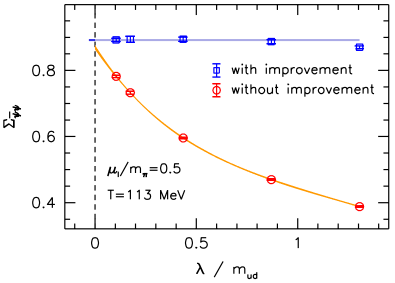

$N_t = 6$

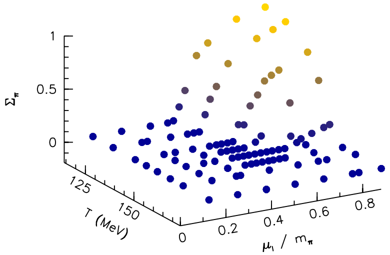

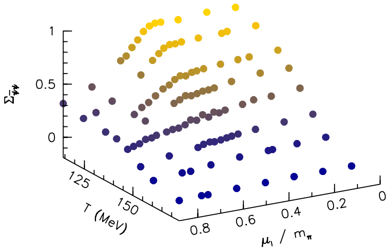

n_I-QCD result - Continuum limit and the $\mu_I - T$ phase diagram

- BEC phase boundary, $\mu_{I,c}(T)$, by points where Σ_π becomes nonzero.
- $\mu_{I,c}(T,a)$, 4^{th} order polynomial in $(T - T_0)$ with $a-$dependent coefficients and $T_0 = 140$ MeV.

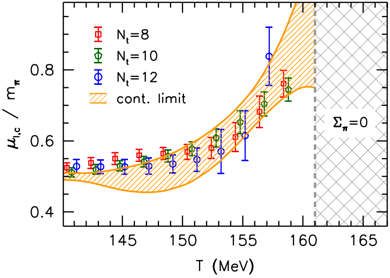

- Chiral crossover $T_{pc}(\mu_I)$, by the inflection points of $\Sigma_{\bar\psi\psi}(T)$
- $T_{pc}(\mu_I, a)$, even-in-μ_I polynomial, including data up to $\mu_{I,c}(0) = m_\pi/2$.

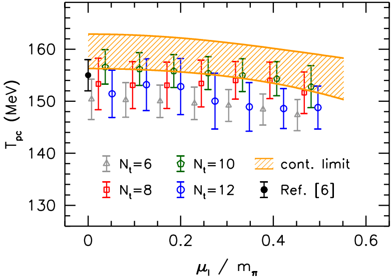

n_I-QCD result - Continuum limit and the $\mu_I - T$ phase diagram

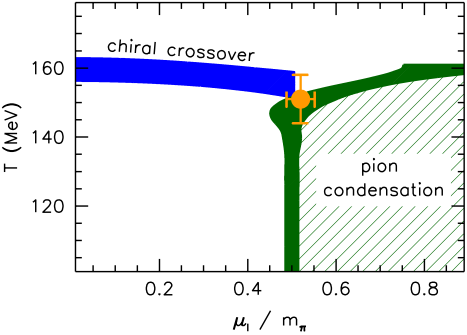

- Chiral crossover transition from $T_{pc}(\mu_I = 0) = 159(4)$ MeV
- Small downward curvature of the $T_{pc}(\mu_I)$ line
- For $T \gtrsim 160$ MeV, no pion condensation up to $\mu_I = 120$ MeV

- Pion condensation boundary at $\mu_{I,c} = m_\pi/2$ up to $T \approx 140\,\text{MeV}$, very flat at higher temperatures
- Two transition lines meet at $\mu_{I,pt} = 70(5)$ MeV in a pseudo-triple point
- From observations at finite a, chiral symmetry restoration and the pion condensation phase boundary coincide for $\mu_I >= \mu_{I,pt} = 70(5)$ MeV

SIGNATURES OF THE BCS PHASE AT HIGH μ_I

[2d complex Dirac spectrum]

BCS phase @ high-μ_I - Motivation: Deconfinement crossover

- Large values of the Polyakov loop within the BEC phase hint to a superconducting ground state with deconfined quarks, the BCS phase
- $T_c^{\mathrm{deconf.}}(\mu_I)$ slowly decreases and the deconfinement crossover smoothly penetrates into the BEC phase
- Scenario where the deconfinement transition connects continuously to the BEC-BCS crossover in the (T, μ_I) phase diagram seems to be favored

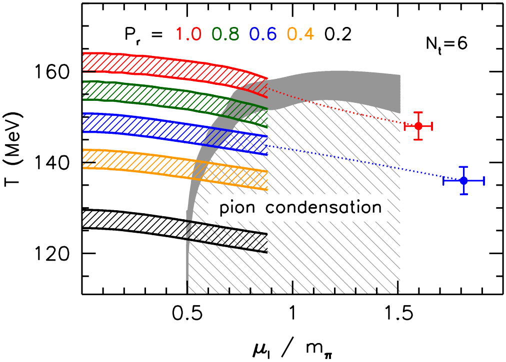

QCD at finite isospin density - The "numeric phase diagram"

- Prediction, from perturbation theory and in a quark meson model, of a superfluid state of u and $\bar{d}$ Cooper pairs (BCS phase) at very high isospin densities and $T = 0$, plausibly connected via an analytical crossover to the a phase with Bose-Einstein condensation of charged pions at $\mu_I >= m_\pi/2$

Son, Stephanov (2001) Adhikari, Andersen, Kneschke (2018)

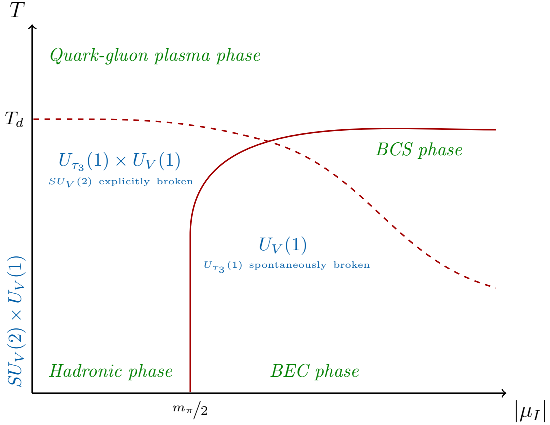

Signatures of the BCS phase from the complex Dirac spectrum

- Banks-Casher relation extensible to the case of complex Dirac eigenvalues for QCD at zero-temperature, nonzero isospin chemical potential
  - The necessary condition for the derivation is the positivity of the fermionic measure ($\rightarrow$ QCD inequalities $\rightarrow$ exclusion of symmetry breaking patterns)
  - For $|\mu_I| \gg \Lambda_{QCD}$ attractive channel between quarks near the Fermi surface lead to diquark pairing of the BCS type
- The density of the complex Dirac eigenvalues at the origin is proportional to the BCS gap squared

$$\Delta^2 = \frac{2\pi^3}{3N_C}\rho(0)$$

Kanazawa, Wettig, Yamamoto (2013)

  - Δ is the BCS gap
  - $\rho(\nu)$ is a 2d spectral density
- BC relations derived considering $\mathcal{Z}(M)$ as function of the quark mass matrix M
  - in the fundamental n_I-QCD theory. Suitable derivatives/limits yield $\rho(0)$
  - in the corresponding effective theory. Suitable derivatives/limits yield Δ^2

Complex spectrum of the Dirac operator

$$\underbrace{[\not{D}(\mu_I)+m_{ud}]\,\psi_n=(\nu_n+m_{ud})\,\psi_n}_{\text{up sector},\mu_I}\xleftrightarrow[\textit{chiral symmetry}]{\eta_5-\textit{hermiticity}}\underbrace{\widetilde{\psi}_n^\dagger\,[\not{D}(-\mu_I)+m_{ud}]=\widetilde{\psi}_n^\dagger(\nu_n^*+m_{ud})}_{\text{down sector},-\mu_I,\widetilde{\psi}_n=\gamma_5\psi_n}$$

- Complex eigenvalues $\nu_n \in \mathbb{C}$
- $[\not{D}(\mu_I), \not{D}^\dagger(\mu_I)] \neq 0$, so left and right eigenvectors of $\not{D}(\mu_I)$ do not coincide
- $\forall$ eigenvalue ν_n in the up sector, complex conjugate ν_n^* in the down sector
- Simulations at nonzero quark mass: instead of $\rho(0)$, we look at $\rho(m + i * 0)$ neglecting corrections at first.

Complex spectrum of $\not{D}(\mu_I) + m_{ud}$ - Measurement & analysis

Measurement

- The spectrum is measured using SLEPc (Scalable Library for Eigenvalue Problem Computations), setting it up to obtain, via the Krylov-Schur method, the eigenvalues of the non-hermitian Dirac operator, which are the closest (in modulo) to the origin ($\sim$150 eigenvalues per configuration).

Analysis

- Two different strategies were developed for the analysis, they consists in extrapolating the 2D density $\rho(\nu)$ to $m + i * 0$, by
  - Evaluating $\rho(\nu)$ in concentric circles centered at $m + i * 0$ and then combining results from different extrapolating Ansätze.
  - Using kernel density estimation (KDE) as a non-parametric way to estimate the multivariate probability density function from the measured spectrum.

Complex spectrum of $\not{D}(\mu_I) + m_{ud}$ - Results, qualitatively

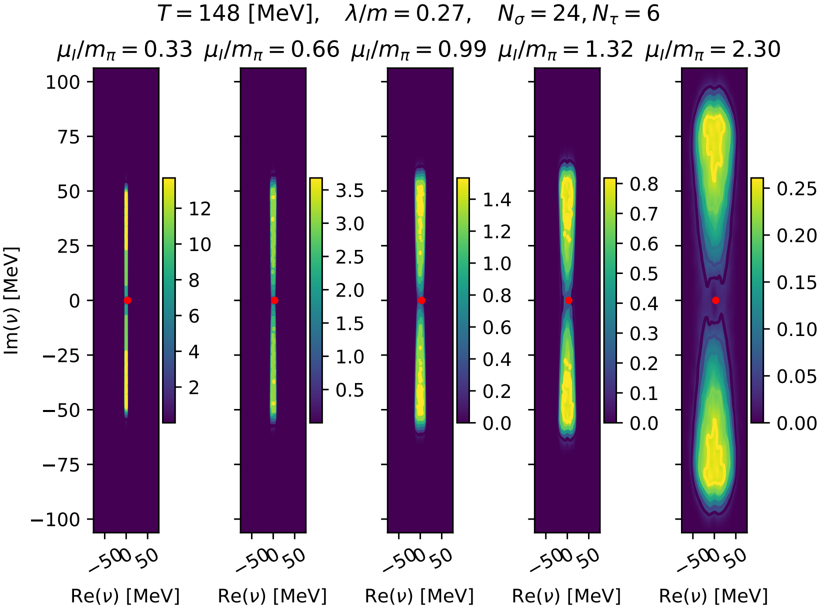

Complex spectrum of $\not{D}(\mu_I) + m_{ud}$ - Results, qualitatively

- Simulations are carried out for physical pion masses, away from the chiral limit, so we try to extract $\rho(m + i0)$
- In the BEC phase the spectrum is wide enough in the real direction to include $m + i0$, hence $\rho(m + i0) \neq 0$
- At $\mu_I < m_\pi/2$ the eigenvalues are clustered along the imaginary axis, hence $\rho(m + i0) = 0$
- At the largest simulated μ_I there is a tendency $\rho(m + i0) \to 0$ due to the eigenvalues drifting away from the real axis.

Complex spectrum of $\not{D}(\mu_I) + m_{ud}$ - Results, quantitatively

- μ_I- and T- dependence of $\rho(m + i0)$ for two different spatial volume sizes

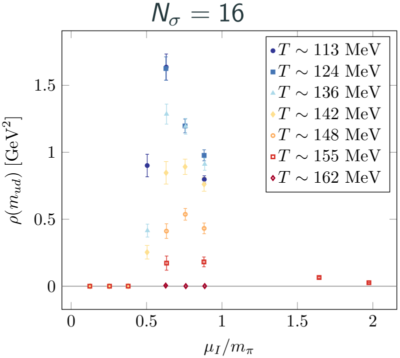

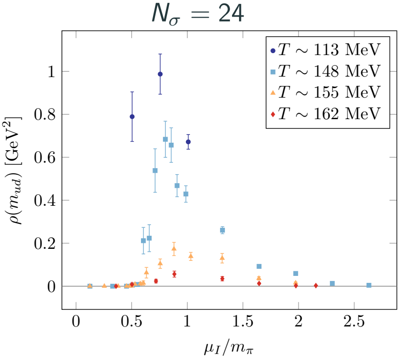

Complex spectrum of $\not{D}(\mu_I) + m_{ud}$ - Results, quantitatively

- Match μ_I- and T- dependence of $\rho(m + i0)$ with the location of the boundary of the BEC phase and with characteristic points of Polyakov loop

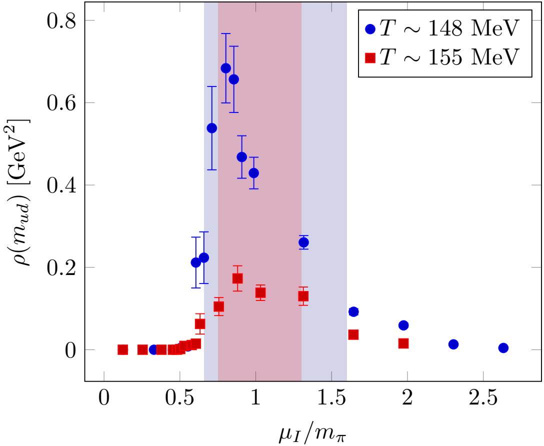

Complex spectrum of $\not{D}(\mu_I) + m_{ud}$ - Results, quantitatively

- Match μ_I- and T- dependence of $\rho(m + i0)$ with the location of the boundary of the BEC phase and with characteristic points of Polyakov loop

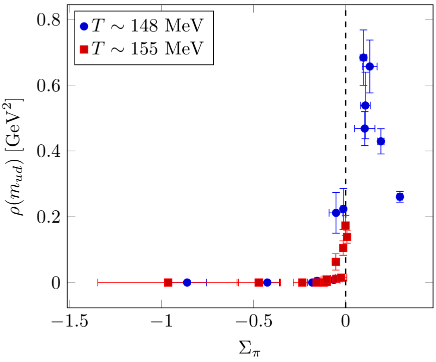

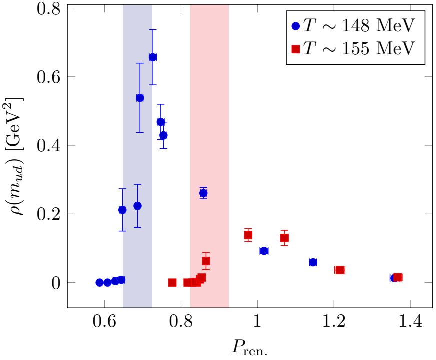

Complex spectrum of $\not{D}(\mu_I) + m_{ud}$ - Results, outlook

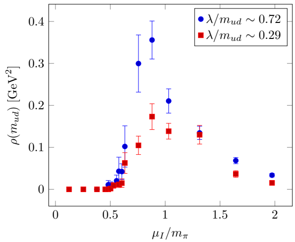

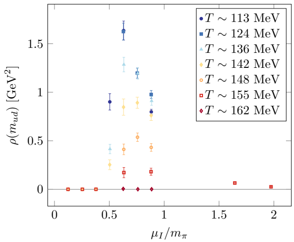

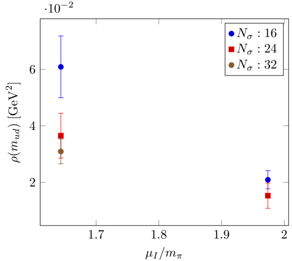

$$a \to 0$$

Complex spectrum of $\not{D}(\mu_I) + m_{ud}$ - Results, outlook

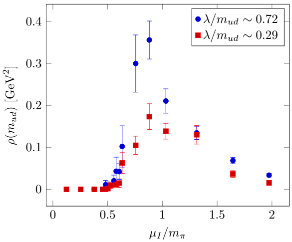

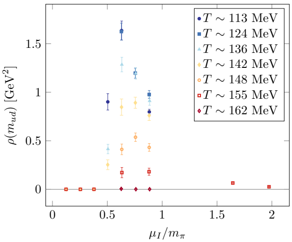

$$V \to \infty \qquad\qquad a \to 0$$

Complex spectrum of $\not{D}(\mu_I) + m_{ud}$ - Results, outlook

$$\lambda \to 0$$

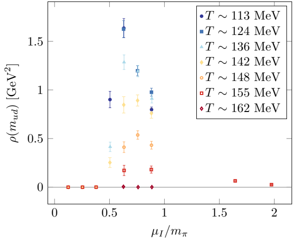

$$V \to \infty$$

$$a \to 0$$

Complex spectrum of $\not{D}(\mu_I) + m_{ud}$ - Results, outlook

$\lambda \rightarrow 0$

$T \rightarrow 0$

$V \rightarrow \infty$

$a \rightarrow 0$

Thank you for your attention!

n_I-QCD on the lattice - No sign problem

- In our partition function $\mathcal{Z} = \int \mathcal{D}U_\mu \, e^{-\beta S_G^{\mathrm{Sym}}} \, (\det \mathcal{M}_{ud})^{1/4} \, (\det \mathcal{M}_s)^{1/4}$

$$\mathcal{M}_{ud} = \begin{pmatrix} \not{D}(\mu_I) + m_{ud} & \lambda\eta_5 \\ -\lambda\eta_5 & \not{D}(-\mu_I) + m_{ud} \end{pmatrix}, \quad \mathcal{M}_s = \not{D}(0) + m_s$$

- $\det \mathcal{M}_s \in \mathbb{R}^+$ due to the standard η_5-hermiticity relation $\eta_5 \mathcal{M}_s \eta_5 = \mathcal{M}_s^\dagger$ with $\eta_5 = \gamma_5^{\mathrm{S}} \otimes \gamma_5^{\mathrm{F}} = (-1)^{n_x+n_y+n_z+n_t}$ equivalent of γ_5 is the local staggered spin-flavor structure
- $\det \mathcal{M}_{ud} \in \mathbb{R}^+$ due to

$$\left.\begin{aligned} \not{D}(\mu_I)\eta_5 + \eta_5 \not{D}(\mu_I) = 0 \\ \eta_5 \not{D}(\mu_I)\eta_5 = \not{D}(-\mu_I)^\dagger \end{aligned}\right\} \Longrightarrow \tau_1 \eta_5 \, \mathcal{M}_{ud} \, \eta_5 \tau_1 = \mathcal{M}_{ud}^\dagger$$

  and

$$\mathcal{M}'_{ud} = B\mathcal{M}_{ud}B = \begin{pmatrix} \not{D}(\mu_I) + m_{ud} & \lambda \\ -\lambda & [\not{D}(\mu_I) + m_{ud}]^\dagger \end{pmatrix}, \quad B = \mathrm{diag}(1, \eta_5)$$

n_I-QCD on the lattice - The $\lambda \to 0$ extrapolation

- The idea is...
  - $\lambda > 0$ triggers pion condensation, but λ is unphysical so a $\lambda \to 0$ extrapolation is needed
- The problems are...
  1. Observables exhibit pronounced λ-dependence
  2. The condition number of the fermion matrix $\kappa(\mathcal{M}_{ud})$ is strongly affected by λ, because λ acts as a I.R. regulator
  3. Fluctuations in the fermion force are regulated/influenced by λ
- Taking the $\lambda \to 0$ limit requires an improvement strategy to be devised
  1. To inhibit the observable's λ dependence
  2. To reduce simulation costs
- The needed improvement is a twofold one concerning both
  - the valence sector $\longrightarrow$ operators modified on the basis of the singular value representation of $\not{D}(\mu_I) + m_{ud}$ to remove explicit dependence on λ
  - the sea sector $\longrightarrow$ configurations reweighted to $\lambda = 0$ (reweighting factor to leading order in λ)

n_I-QCD on the lattice - Improvement in the sea sector

- λ-dependence from the path integral measure that defines $\langle\mathcal{O}\rangle_\lambda$
- Manipulate the distribution of configurations by introducing the reweighting factors to get rid of λ-dependence of $\det\mathcal{M}_{ud}$

$$\langle\mathcal{O}\rangle_{\lambda=0} = \frac{\langle\mathcal{O}\,W(\lambda)\rangle_{\lambda>0}}{\langle W(\lambda)\rangle_{\lambda>0}},$$

$$W(\lambda) \equiv \frac{\det\left[|\not{D}(\mu_I)+m_{ud}|^2\right]^{1/4}}{\det\left[|\not{D}(\mu_I)+m_{ud}|^2+\lambda^2\right]^{1/4}},$$

- Mimic the distribution that would have been obtained via at $\lambda = 0$
- The need for $W(\lambda)$ only at small λ values allows us the approximation

$$\log W(\lambda) = -\frac{\lambda V}{2T}\pi^{\pm} + \mathcal{O}(\lambda^4) \equiv \log W_{\mathrm{LO}}(\lambda) + \mathcal{O}(\lambda^4)$$

- The reweighting of an observable, to leading order in λ, involves the exponential of the pion condensate (measured at $\lambda > 0$) $\rightarrow$ no costs!

n_I-QCD on the lattice - Singular value representation $\not{D}(\mu_I) + m_{ud}$

$$\underbrace{[\not{D}(\mu_I)+m_{ud}]\,\psi_n=(\nu_n+m_{ud})\,\psi_n}_{\text{up sector},\mu_I} \xleftrightarrow[\text{chiral symmetry}]{\eta_5-\text{hermiticity}} \underbrace{\widetilde{\psi}_n^\dagger\,[\not{D}(-\mu_I)+m_{ud}]=\widetilde{\psi}_n^\dagger(\nu_n^*+m_{ud})}_{\text{down sector},-\mu_I,\widetilde{\psi}_n=\gamma_5\psi_n}$$

- $[\not{D}(\mu_I), \not{D}^\dagger(\mu_I)] \neq 0$, so left and right eigenvectors of $\not{D}(\mu_I)$ do not coincide
- $\forall$ eigenvalue ν_n in the up sector, complex conjugate ν_n^* in the down sector
- Hermitian operator by taking the modulus squared of $\not{D}(\mu_I) + m_{ud}$ and considering the eigenproblem

$$[\not{D}(\mu_I) + m_{ud}]^\dagger[\not{D}(\mu_I) + m_{ud}]\,\varphi_n = \xi_n^2\,\varphi_n$$

the square root of the eigenvalues of which are the singular values ξ_n

n_I-QCD on the lattice - $\langle\pi^\pm\rangle$ improvement in the valence sector

- $\langle\pi^\pm\rangle$ satisfies a Banks-Casher type relation for $\lambda \to 0$ in analogy with the quark condensate in the chiral limit
- Singular value representation of the pion condensate

$$\begin{aligned}\langle\pi^\pm\rangle &= \frac{T}{2V}\,\mathrm{tr}\,\frac{\lambda}{|\not{D}(\mu_I)+m_{ud}|^2+\lambda^2}\\ &\xrightarrow[\text{in the basis of }\varphi_n]{|\not{D}(\mu_I)+m_{ud}|^2\text{diagonal}} \frac{\lambda T}{2V}\left\langle \sum_n (\xi_n^2+\lambda^2)^{-1}\right\rangle\\ &\xrightarrow{V\to\infty} \frac{\lambda}{2}\left\langle \int \mathrm{d}\xi\,\rho(\xi)(\xi^2+\lambda^2)^{-1}\right\rangle\\ &\xrightarrow{\lambda\to 0} \frac{\pi}{4}\langle\rho(0)\rangle\end{aligned}$$

- Density of singular values $\langle\rho(\xi)\rangle = \lim_{V\to\infty}\frac{T}{V}\left\langle\sum_n \delta(\xi-\xi_n)\right\rangle$
- $\langle\pi^\pm\rangle \neq 0$ equivalent to accumulation of near-zero ξ_n of $\not{D}(\mu_I)+m_{ud}$

n_l-QCD on the lattice - $\langle \pi^{\pm} \rangle$ improvement in the valence sector

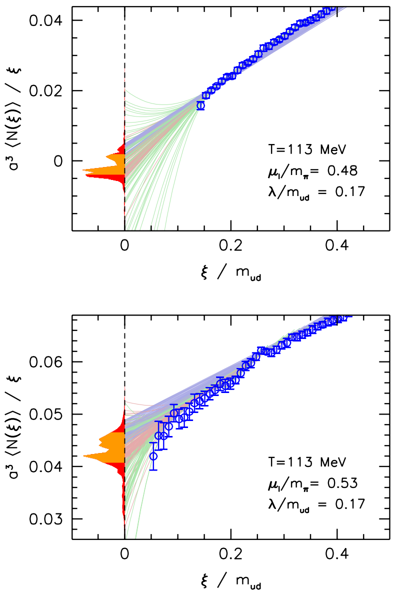

- Krylov-Schur to obtain lowest $\mathcal{O}(100)$ ξ_n
- Histogram for the integrated spectral density

$$N(\xi) = \int_0^{\xi} \mathrm{d}\xi' \rho(\xi')$$

- Statistical error of $N(\xi)$ in each bin via jackknife
- Polynomial fits to extrapolate $N(\xi)/\xi$ down to zero and get $\rho(0)$
- Results used to build another histogram, the median of which gives $\rho(0)$
- Observed emergence of a nonzero pion condensate in the BEC phase

n_I-QCD on the lattice - $\langle\bar{\psi}\psi\rangle$ improvement in the valence sector

- Spectral representation for $\langle\bar{\psi}\psi\rangle$ in the basis of the φ_n modes

$$\langle\bar{\psi}\psi\rangle^{(N)} = \frac{T}{2V}\mathrm{Re\ tr}\,\frac{\not{D}(\mu_I)+m_{ud}}{|\not{D}(\mu_I)+m_{ud}|^2+\lambda^2} = \frac{T}{2V}\sum_n^{(N)}\frac{\mathrm{Re}\varphi_n^\dagger[\not{D}(\mu_I)+m_{ud}]\varphi_n}{\xi_n^2+\lambda^2}$$

- $[\not{D}(\mu_I)+m_{ud}]$ not diagonal in such basis $\rightarrow$ various matrix elements needed
- λ dependence accessed via

$$\delta_{\bar{\psi}\psi}^{(N)} \equiv \bar{\psi}\psi^{(N)}(\lambda) - \bar{\psi}\psi^{(N)}(\lambda=0) = \frac{T}{2V}\sum_n^{(N)}\mathrm{Re}\varphi_n^\dagger[\not{D}(\mu_I)+m_{ud}]\varphi_n\cdot\left(\frac{1}{\xi_n^2+\lambda^2}-\frac{1}{\xi_n^2}\right)$$

- $\delta_{\bar{\psi}\psi}$ dominated by the λ dependence of the terms involving the lowest ξ_n
- explicit $\lambda\rightarrow 0$ extrapolation in the operator for only the first N low modes

$$\langle\bar{\psi}\psi\rangle = \left\langle\bar{\psi}\psi-\delta_{\bar{\psi}\psi}^N\right\rangle + \left\langle\delta_{\bar{\psi}\psi}^N\right\rangle \quad\Longrightarrow\quad \lim_{\lambda\to 0}\langle\bar{\psi}\psi\rangle = \lim_{\lambda\to 0}\left\langle\bar{\psi}\psi-\delta_{\bar{\psi}\psi}^N\right\rangle$$

n_I-QCD on the lattice - $\langle \bar{\psi}\psi \rangle$ improvement in the valence sector

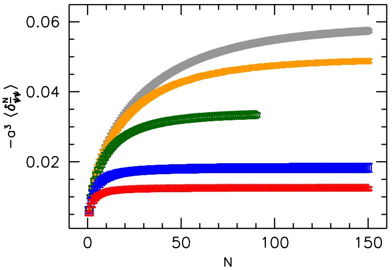

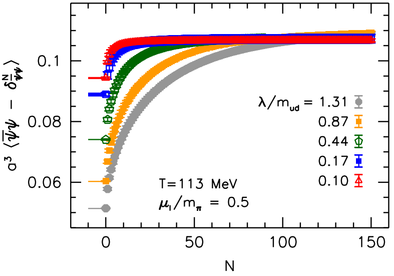

- $\delta^N_{\bar{\psi}\psi}$, calculated using the N lowest singular values, on ensembles with various values of λ
- Improvement achieved via the subtraction

$$\langle \bar{\psi}\psi \rangle = \left\langle \bar{\psi}\psi - \delta^N_{\bar{\psi}\psi} \right\rangle + \left\langle \delta^N_{\bar{\psi}\psi} \right\rangle$$

- improvement will be efficient if N is large enough to ensure that $\delta^N_{\bar{\psi}\psi} \approx \delta_{\bar{\psi}\psi}$
- Optimal value for N balance between improvement and computational cost
- No significant λ dependence for $N \gtrsim 100$ for all ensembles